

This is the accepted manuscript of the contribution published as:

David, C., Schmid, A., Adrian, L., Wilde, A., Bühler, K. (2018):

Production of 1,2-propanediol in photoautotrophic *Synechocystis* is linked to glycogen turn-over

Biotechnol. Bioeng. **115** (2), 300 – 311

The publisher's version is available at:

<http://dx.doi.org/10.1002/bit.26468>

**Production of 1,2-propanediol in photoautotrophic *Synechocystis* is linked to glycogen
turn-over[†]**

Running title: 1,2-propanediol from *Synechocystis* PCC6803

Christian David¹, Andreas Schmid¹, Lorenz Adrian², Annegret Wilde³, Katja Bühler^{1,*}

¹ Department Solar Materials, Helmholtz Centre for Environmental Research - UFZ, Leipzig,
Germany

² Department Isotope-Biogeochemistry, Helmholtz Centre for Environmental Research -
UFZ, Leipzig, Germany

³ Institute of Biology III, University of Freiburg, Freiburg, Germany

***Correspondence to:**

Katja Bühler

Department Solar Materials, Helmholtz Centre for Environmental Research - UFZ

Permoserstraße 15, 04318 Leipzig, Germany

telephone: +49 341 235 - 46 83

fax: +49 341 235 - 45 1286

email: katja.buehler@ufz.de

[†]This article has been accepted for publication and undergone full peer review but has not been through the copyediting, typesetting, pagination and proofreading process, which may lead to differences between this version and the Version of Record. Please cite this article as doi: [10.1002/bit.26468]

Additional Supporting Information may be found in the online version of this article.

This article is protected by copyright. All rights reserved

Received June 7, 2017; Revision Received September 3, 2017; Accepted October 5, 2017

Abstract

We utilized a photoautotrophic organism to synthesize 1,2-propanediol from carbon dioxide and water fueled by light. A synthetic pathway comprising *mgsA* (methylglyoxal synthase), *yqhD* (aldehyde reductase), and *adh* (alcohol dehydrogenase) was inserted into *Synechocystis* sp. PCC6803 to convert dihydroxyacetone phosphate to methylglyoxal, which is subsequently reduced to acetol and then to 1,2-propanediol. 1,2-propanediol could be successfully produced by *Synechocystis*, at an approximate rate of $55 \mu\text{mol h}^{-1} \text{g}_{\text{CDW}}^{-1}$. Surprisingly, maximal productivity was observed in the stationary phase. The production of 1,2-propanediol was clearly coupled to the turn-over of intracellular glycogen. Upon depletion of the glycogen pool, product formation stopped. Reducing the carbon flux to glycogen significantly decreased final product titers. Optimization of cultivation conditions allowed final product titers of almost 1 g L^{-1} (12 mM), which belongs to the highest values published so far for photoautotrophic production of this compound. This article is protected by copyright. All rights reserved

Keywords:

Cyanobacteria, 1, 2 - propanediol, storage compound, photosynthesis, autotrophic production, biocatalysis

1. Introduction

The limited availability of fossil carbon-based feedstocks calls for alternative sustainable solutions for the production of energy carriers and chemicals. In this context, photoautotrophic organisms have received increasing attention during the last decade, as they generate valuable compounds from CO₂ and water fueled by sunlight. Numerous studies have demonstrated the potential of this approach, showing proof of concept for various products ranging from alcohols to organic acids, as well as alkanes, ethylene, and some fine chemicals (extensively reviewed by Angermayr et al., 2015; Oliver and Atsumi, 2014; Savakis and Hellingwerf, 2015). Despite the wide variety of products accessible using photoautotrophic organisms, successful implementation of such a concept on an industrial level is rarely achieved. Due to the insufficient understanding of the highly complex cyanobacterial metabolism a well-established production strain, like *E.coli*, is so far not available for photoautotrophic microbes. Prevailing challenges are manifold and include low biocatalytic activity and stability of the whole-cell photo-biocatalyst, as well as insufficient product titer (Savakis and Hellingwerf, 2015; Zhou et al., 2016).

In the present study, we investigate the synthesis of 1,2-propanediol utilizing a recombinant *Synechocystis* sp. PCC 6803 strain (hereafter referred to as *Synechocystis*), focusing especially on its physiology and production profile. 1,2-Propanediol, more commonly known as propylene glycol is a bulk chemical with a high market volume that is applied in chemical, food, cosmetic and pharmaceutical industries (Bridgwater et al., 2010). Every year, 2.18 million tons of 1,2-propanediol is produced from petroleum-based feedstock. The negative environmental impact of the conventional 1,2-propanediol production in combination with the finite nature and instability of fossil carbon supply is anticipated to drive the demand for bio-based 1,2-propanediol on a global scale (Saxena et al., 2010). A three step heterologous pathway was introduced into *Synechocystis* for the fermentative synthesis of 1,2-propanediol

(Figure 1), building on the study of Li and coworkers with *Synechococcus elongatus* PCC 7942 (Li and Liao, 2013). Methylglyoxal synthase converts the precursor dihydroxyacetone phosphate (DHAP) into methylglyoxal (Hopper and Cooper, 1971). Subsequently, methylglyoxal is reduced to acetol and then to 1,2-propanediol utilizing a methylglyoxal reductase and a secondary alcohol dehydrogenase, respectively. During the reduction of methylglyoxal to 1,2-propanediol two reduced nicotinamide adenine dinucleotide phosphates (NADPH) are oxidized. Special focus was placed on the bottlenecks occurring during the production phase. Synthesis of 1,2-propanediol was clearly uncoupled from growth and commenced in the transition from growth to stationary phase. We could show that production of 1,2-propanediol is linked to glycogen turn-over and final product titers correlate with the available cellular glycogen. Based on these findings optimization of cultivation conditions allowed final product titers of 950 mg/L, which are the highest values achieved so far for photoautotrophic production of this compound.

2. Materials and methods

Chemicals and reagents

All chemicals used were obtained from AppliChem (Darmstadt, Germany), Sigma Aldrich (Steinheim, Germany), or CarlRoth (Karlsruhe, Germany) unless stated otherwise and were of the highest purity available. Custom synthesized oligonucleotides were purchased by Eurofins Genomics GmbH (Ebersberg, Germany). Restriction enzymes, ligases, exonucleases, dNTPs and Phusion polymerase were provided by New England Biolabs (Ipswich, Massachusetts, USA) and Fermentas/Thermo Fisher Scientific (Waltham, MA, USA).

Cultivation of strains

All bacterial strains and plasmids used in this study are listed in table I. *Escherichia coli* DH5 α was used for cloning purposes and plasmid storage. *E. coli* cultures were started from cryo stocks, which were transferred on LB agar (Bertani, 1951). A single colony from such a plate

was used to inoculate 5 mL of LB liquid culture containing the respective antibiotics, where applicable. Cells were incubated at 37°C. *E. coli* strains were stored at -80°C in 15% glycerol. The cyanobacterial strain *Synechocystis* sp. PCC6803 (herein called *Synechocystis*; Stanier et al., 1971) was obtained from the Pasteur Culture Collection of Cyanobacteria (PCC, Paris, France).

BG11 medium (Stanier et al., 1971) or YBG11 medium (Shcolnick et al., 2007) was used for cultivation of *Synechocystis*. Agar plates containing the respective antibiotics (either Km⁵⁰, Cm¹⁵, or a combination of both, where the superscript refers to the respective antibiotic concentration in µg mL⁻¹) were inoculated from a cryo stock and cultivated for 10 days under 25 µmol m⁻² s⁻¹ photosynthetically active radiation, ambient CO₂, 30°C, and 75% humidity in a polyklima incubator (Polyklima, Freising, Germany). Single colonies were transferred to fresh agar plates and spread to obtain enough biomass to inoculate YBG11 containing 50 mM HEPES buffer. 50 mL of liquid *Synechocystis* cultures were grown in 250 ml baffled shaking flasks under increasing light intensity, 2% CO₂, 30°C, 150 rpm, and 75% humidity in an INFORS Multitron photosynthesis plus incubator (INFORS, Bottmingen, Switzerland), equipped with light-emitting diodes. Cultures were inoculated to an OD_{750nm} of 0.2 for the main experiments. For long-term storage the strains were frozen in YBG11 medium containing 8% DMSO at - 80°C.

Construction of the 1,2-propanediol pathway in *Synechocystis*

The genes *mgsA*, *yqhD*, and *adh*, enabling the production of 1,2-propanediol from DHAP, were integrated into the neutral site *slr0168* (Williams, 1988) of *Synechocystis* by double homologous recombination. Therefore, the homologous regions (550 bp), for recombination were amplified from genomic DNA applying primers homI_fwd, homI_rev, homII_fwd, and homII_rev. The primers used for PCR amplification of all fragments are listed in table II. Genomic DNA was isolated using the peqGOLD Bacterial DNA Mini Kit (VWR Peqlab,

Darmstadt, Germany) upon cell disruption using a bead mill (0.2 μm glass beads, 8,000 rpm, 3 cycles a 30 s). The two derived PCR products were subsequently subcloned into pBluescriptII SK(+) (Agilent technologies, Santa Clara, CA, USA) by Gibson assembly (Gibson et al., 2009) using restriction sites for KpnI, XhoI, SacI, and SacII, respectively. Digestion of plasmid DNA was carried out at 37°C for 16 h. The TRC promoter system was amplified from pSEVA234 (SEVA collection, Centro Nacional de Biotecnología, Madrid, Spain) using *lacIQTRC_fwd* and *lacIQTRC_rev* and inserted between the two homologous regions using restriction sites XhoI and SacII, resulting in pBS_slr0168::TRC.

In the following, the genes *mgsA* and *yqhD* were amplified using *E.coli* MG1655 genomic DNA and primers *mgsA_fwd*, *mgsA_rev*, *yqhD_fwd*, and *yqhD_rev*. The codon optimized *adh* gene of *Clostridium beijerinckii* (Yan et al., 2009) was synthesized (Eurofins Genomics GmbH, Ebersberg, Germany) and amplified from the obtained vector pEX-K4_ *adh* using *CBsadh_fwd* and *CBsadh_rev*. The respective forward primers included the same ribosomal binding site for each gene (Table II, RBS are dashed underlined). The three derived fragments were combined by overhang extension PCR and cloned into pBS_slr0168::TRC using the Gibson assembly protocol and the restriction enzyme NotI. Fragments and PCR products were identified and selected by agarose gel electrophoresis, and purified using a NucleoSpin Gel and PCR Clean-up kit (Macherey-Nagel, Düren, Germany). Gibson assembly was carried out at 50°C for 60 min using a Mastercycler pro PCR System (Eppendorf, Hamburg, Germany). Competent *E. coli* DH5 α were transformed with the assembled DNA fragments by electroporation. Plasmids were isolated from LB overnight cultures using a peqGOLD Plasmid Miniprep Kit (VWR Peqlab, Darmstadt, Germany) and sequenced (Eurofins Genomics GmbH, Ebersberg, Germany). The resulting vector pBS_slr0168::TRC:*adh:yqhD:mgsA* was used to transform the strains *Synechocystis* and *Synechocystis* ΔglgC_{hw} (kindly donated by the Hellingwerf lab (Van der Woude et al., 2014)) creating the recombinant strains *Synechocystis* PG and *Synechocystis*

ΔglgC_{hw} PG. Complete segregation of the mutant allele in the created *Synechocystis ΔglgC_{hw}* PG strain was reached by continuous cultivation on solid medium with increasing antibiotic concentrations and was verified by PCR with isolated genomic DNA as template.

Construction of the *glgC* knockout in *Synechocystis*

The *glgC* gene was replaced by a gene encoding streptomycin resistance *aadA* by double homologous recombination. Homologous regions for recombination (~850 bp) were amplified from genomic DNA applying primers *glgC_cut1_fwd*, *glgC_cut1_rev*, *glgC_cut2_fwd*, and *glgC_cut2_rev* (Table II). *aadA* was amplified from pSEVA451 using the primers *Sm_fwd* and *Sm_rev*. All three PCR products were subsequently subcloned into pBR322 via three fragment Gibson assembly (Gibson et al., 2009) using the restriction site for EcoRI. The resulting vector pBR322_*glgC_cut* was used to transform the strains *Synechocystis* and *Synechocystis* PG creating the recombinant strains *Synechocystis ΔglgC* and *Synechocystis ΔglgC* PG. Complete segregation of the mutant allele in the created *Synechocystis ΔglgC* strain was reached by continuous cultivation on solid medium with increasing antibiotic concentrations and was verified by PCR with isolated genomic DNA as template.

Growth determination and light quantification

Planktonic cell growth was quantified by turbidity (OD₇₅₀, Libra S11, Biochrom Ltd, Cambridge, UK) and coulter counter measurements according to standard procedures (Multisizer 3, 20 μm aperture, Beckman Coulter, Brea, California, United States). For the determination of cell dry weight (CDW) cultures samples were centrifuged and dried at 80°C. Photosynthetically active radiation (PAR) was determined with a MQS-B mini quantum sensor coupled to an ULM-500 light meter (Heinz Walz GmbH, Effeltrich, Germany).

Determination of glycogen and polyhydroxybutyrate content

For the determination of the concentration of storage compounds, a sample of 2 mL of the respective culture was centrifuged (17000 × g, 10 min, 4°C). The pellet was washed once in

ultra clean water and stored at -80°C . Isolation of glycogen was carried out according to a protocol modified from Gründel et al (Gründel et al., 2012). Briefly, the cell pellet was resuspended in $500\ \mu\text{L}$ of $30\%_{\text{w/v}}$ KOH in a 2-mL Eppendorf cup and afterwards incubated at 95°C , 600 rpm, for 2 h in a thermoshaker. The glycogen was precipitated by the addition of 1.5 mL of ice-cold ethanol and subsequent incubation at -20°C for 4 h. Glycogen was received by centrifugation ($17000 \times g$, 10 min, 4°C), washed once with 75% ethanol and once with 98% ethanol. The remaining ethanol was evaporated in a thermoshaker at 65°C for 2 h. The glycogen amount was determined with a fluorimetric glycogen assay (glycogen assay kit, Cayman chemical, item no. 7000480) according to the distributors' protocol.

Polyhydroxybutyrate (PHB) was determined as described previously (Taroncher-Oldenburg and Stephanopoulos, 2000). The cell pellet was dried in a thermoshaker (95°C , 6 h), resuspended in $100\ \mu\text{L}$ of concentrated sulfuric acid, and boiled at 95°C for 2 h in a thermoshaker. After dilution with $400\ \mu\text{L}$ of ultra clean water and centrifugation ($17000 \times g$, 10 min, 4°C), the supernatant was analyzed using HPLC (Thermo Fisher Scientific, Waltham, MA, USA), equipped with a Aminex HPX-87H column ($300 \times 7.8\ \text{mm}$, Bio-Rad Laboratories GmbH, Hercules, California, USA) and refraction index detector. Commercially available PHB (Sigma Aldrich, 363502) was used as a standard compound and handled accordingly.

Determination of 1,2-propanediol, acetol, methylglyoxal, nitrate, and phosphate

Supernatant of the *Synechocystis* cultures was analyzed with a Dionex Ultimate 3000 high pressure liquid chromatography system (Thermo Fisher Scientific, Waltham, MA, USA) equipped with a refraction index detector and an Aminex HPX-87H column ($300 \times 7.8\ \text{mm}$, Bio-Rad Laboratories GmbH, Hercules, California, USA). The flow rate was set to $1\ \text{mL}\ \text{min}^{-1}$ with 5 mM sulfuric acid as the eluent. Standard curves for all compounds were prepared to quantify the product concentrations in the supernatant of the cultures.

Identification of 1,2-propanediol

Two hundred microliters of culture supernatant was dried at 80°C, and the remaining compounds were resuspended in acetonitrile and derivatized with 1-((*tert*-butyldimethylsilyl)oxy)propan-2-ol. Obtained samples were separated on a Trace 1310 GC equipped with a TG-5MS column (40 m) and analyzed on an ISQ LT MS (Thermo Fisher Scientific, Waltham, MA, USA). The obtained spectra were compared to the derivatized standard compound 1,2-propanediol (min. 99,5%, Bernd Kraft GmbH, Duisburg, Germany).

Northern blot

For northern blot analysis 10-25 mL of culture were filtrated through a Supor-800 Filter (Grid, 0.8 μ m, 47 mm, Pall Life Sciences, Michigan, USA). Filter and retained biomass were dissolved in 1.6 mL of PGTX solution (Pinto et al., 2009) and frozen in liquid nitrogen. Samples were than thawed and incubated at 95°C for 5 minutes. Then, 200 μ L of pre-cooled 1-bromo-3-chloro-propane (BCP) was added to the samples. Phases were separated by centrifugation (4700 \times g, 15 min, 4°C) and the aqueous phase was again extracted with BCP. RNA was precipitated overnight (-20°C) with the addition of isopropanol to the aqueous phase. After centrifugation, the RNA pellet was washed with 75% precooled ethanol and dried at room temperature. Three micrograms of total RNA was separated by electrophoresis on 1.3% denaturing agarose gels, blotted onto Roti-Nylon plus (Roth) membranes and hybridized as described (Dienst et al., 2008). Hybridization probes were generated either by *in vitro* transcription of PCR fragments from the T7 promoter in the presence of [α -³²P]UTP using a T7 polymerase Maxiscript kit (Ambion) for *mnpB* or by labeling DNA fragments with [α -³²P]CTP using the Rediprime II DNA labeling system (GE Healthcare Life Sciences). Signals were detected and analyzed on a Phosphor Imager (Typhoon FLA 9500, GE Healthcare Life Sciences). The oligonucleotides used for PCR amplification are listed in table II. DNA hybridization probes covered the complete coding region of the respective genes.

Mass spectrometric detection and quantification of proteins

Protein expression from the recombinant pathway genes was analyzed from 2 mL samples containing 10^8 *Synechocystis* PG cells per mL. Samples were harvested by centrifugation, lysed by bead beating, digested with trypsin and derivatized with iodoacetamide, all as described previously (Schippe et al., 2013). Samples were subsequently analysed by nano liquid chromatography linked to an Orbitrap mass spectrometer (nLC–MS/MS) on an Orbitrap Fusion instrument (Thermo Fisher Scientific) equipped with a nanoUPLC system (nanoAcquity, Waters) as reported (Marco-Urrea et al., 2011). Peptide identification was based on the protein sequences derived from *Synechocystis* PCC6803 genome (accession number NC_000911.1) and the sequences of *mgsA* (WP_000424181.1), *yqhD* (NP_417484.1) and *adh* (WP_077844196.1). All calculations were done with ProteomeDiscoverer Version 2.2 (Thermo) with SequestHT as the search engine using precursor and fragment mass tolerances of 3 ppm and 0.6 Da, respectively. The peptide identification threshold was set at a false discovery rate (FDR) of 0.01 based on the q-values comparing hits to target and decoy databases. The ‘Minora Feature Detector’ node, the ‘Feature Mapper’ node and the ‘Precursor Ions Quantifier’ node implemented in ProteomeDiscoverer V2.2 was used for label-free quantification on the basis of the intensities of precursor mass spectrometric traces and using the GAP-DH from *Staphylococcus aureus* as an internal standard. Relative abundance ranks of proteins were computed in Microsoft Excel on the basis of the label-free quantification output.

3. Results

Growth of *Synechocystis* PG is unaffected by recombinant gene expression

To elucidate how the recombinant genes influenced the physiology of the 1,2-propanediol producing strain *Synechocystis* PG initial shaking flask experiments have been conducted. Growth phases were distinguished as described by Schuurmans (Schuurmans et al., 2017).

Synechocystis PG and the wild type showed no significant differences in growth during the exponential, linear, and late growth phase (Figure 2A). However, differences appeared when growth ceased. For the wildtype strain a stable OD_{750nm} value was observed during the stationary phase, whereas the OD_{750nm} of the PG strain decreased from 14 to 10 within 5 days. This was also reflected in a decrease in CDW of approximately 0.4 g_{CDW} L⁻¹. Applying a light regime, starting with 25 μmol m⁻² s⁻¹ and increasing up to 200 μmol m⁻² s⁻¹ over cultivation time and elevated CO₂ concentrations (2%) enabled an exponential growth phase up to an OD_{750nm} of 4 (0.66 g_{CDW} L⁻¹) with a growth rate of 0.031 h⁻¹. Thereafter, the culture grew linear up to an OD_{750nm} of 14 (~2.2 g_{CDW} L⁻¹) until growth ceased completely. Growth of the recombinant strain was not impaired by the expression of the heterologous genes.

1,2-propanediol formation mainly in the stationary phase

Functionality and productivity of the heterologous pathway were investigated in shaking flask experiments. Formation of 1,2-propanediol was detected in the supernatant of the culture during the late and stationary growth phase of the recombinant strain, but not during the exponential and linear growth phases (Figure 2B). Induction of the TRC promoter with isopropyl β-D-1-thiogalactopyranoside (IPTG) did not lead to an increased product formation rate, indicating leaky expression, as already reported for the TRC promoter in *Synechocystis* (Huang et al., 2010). Under photoautotrophic standard conditions (constant 50 μmol m⁻² s⁻¹, ambient CO₂) up to 3 mM (228 mg L⁻¹, 9 mmol_C L⁻¹) of 1,2-propanediol accumulated in the culture supernatant (data not shown). With an optimized growth protocol applying an elevated CO₂ concentration of 2% and increasing light intensity up to 200 μmol m⁻² s⁻¹ a final titer of 12 mM (900 mg L⁻¹, 36 mmol_C L⁻¹) 1,2-propanediol was achieved, with a peak volumetric production rate of 2.8 mM day⁻¹, representing a maximal specific activity of 55 μmol h⁻¹ g_{CDW}⁻¹.

¹. Only minor amounts of acetol (<1 mM) and no methyl glyoxal were detected. The production of 1,2-propanediol was verified by gas chromatography mass spectrometry (GC-MS).

Phosphate limitation stalls growth of *Synechocystis* strains in YBG11 medium

The observation that product formation occurs only during transition to and within the stationary phase raised the question how the activity of the recombinant pathway is related to cell growth. A special focus was thus placed on identifying limiting factors responsible for growth arrest. As carbon dioxide and light were supplied continuously, one component of the growth medium YBG11 might have become limiting. YBG11 contains 17.5 mM sodium nitrate and 0.175 mM dipotassium hydrogen phosphate as nitrogen and phosphate source, respectively. HPLC analysis of the supernatant of *Synechocystis* and *Synechocystis* PG cultures during cultivation revealed that when the cultures enter the stationary phase nitrate is still present in the supernatant (data not shown). In contrast, phosphate cannot be detected in the culture broth after the early growth phase (initial 5 days) of the culture (YBG11, Figure 3C). Cultures of *Synechocystis* PG were therefore grown in YBG11 medium containing different amounts of dipotassium hydrogen phosphate (0, 25, 50, 75, 100, 150, and 200% of the phosphate amount originally present in YBG11) (Figure 3A). Final biomass titers correlated linearly between 0 and 100% of added phosphate (Figure 3D). A further increase in phosphate availability only had a slight effect on biomass titers. The maximum OD value reached was 16 at 150% and 200% added phosphate. This indicates that another component of the medium became limiting at that point. Product formation was heavily influenced by the phosphate concentration. Significant amounts of product could only be detected for cultures grown in media containing 100% phosphate or more (Figure 3B). The maximum product amount of 9 mM (685 mg L⁻¹, 27 mmol_C L⁻¹) 1,2-propanediol was measured for medium supplied with 100% phosphate. At concentrations exceeding 100% phosphate, the productivity for 1,2-propanediol formation decreased significantly, indicating an inhibitory effect on the respective

enzyme systems. This provided evidence that growth and productivity of *Synechocystis* in YBG11 is initially strongly influenced by the presence of phosphate. A phosphate limitation is likely to initiate the entrance of the cells into the stationary phase under the conditions applied. Although relieving this limitation leads to higher biomass titers, it concomitantly results in significantly lower 1,2-propanediol concentrations. Apart from nitrogen, phosphate, CO₂ and light, no other compound has been evaluated for possible growth limitation in this study.

1,2-propanediol production is linked to glycogen turn-over

1,2-propanediol production starts within the late growth phase. The necessary carbon and energy for the synthesis of 1,2-propanediol may thus be derived either directly from the Calvin cycle or indirectly from the intracellular accumulated storage compounds polyhydroxybutyrate (PHB) or glycogen. To elucidate the interrelation of storage compounds and 1,2-propanediol production, the intracellular glycogen and PHB pools have been monitored throughout the cultivation of *Synechocystis* PG and the wildtype strain (Figure 2B). PHB was not detected, whereas the glycogen concentration reached a maximum of 18 mmol C L⁻¹ (~24% of CDW) in the wild type. Notably the glycogen pool was not turned over in the stationary phase, which is strikingly different in the recombinant strain *Synechocystis* PG. Here, glycogen accumulated to approximately 18% of the CDW and then decreased to zero during the production phase. The decrease in biomass concentration to 0.4 g L⁻¹ during the production phase fits precisely the amount of glycogen consumed. A decrease of the OD value due to cell lysis can be excluded, as also the cell numbers have been determined via Coulter Counter cell count (Figure 5A). From these findings, we conclude that the decline in biomass is due to glycogen turn-over. After the glycogen pool was depleted, no more 1,2-propanediol formation could be observed. To further elucidate the importance of the glycogen pool for 1,2-propane diol production the strain *Synechocystis* Δ*glgC* PG was designed. Shaking flask cultivations were performed with *Synechocystis* PG and Δ*glgC* PG. The Δ*glgC* PG strain grew significantly slower than the PG

strain and produced about 30% less 1,2-propane diol (Figure 4). However, although *glgC* was apparently deleted, there are indications that glycogen is still produced, as we observe the same decrease in the growth curve during the stationary phase as in the PG strain, which is attributed to glycogen turnover. Notably, the same experiment performed with a *Synechocystis* sp. PCC6803 Δ *glgC* mutant kindly donated from the Hellingwerf lab (Van der Woude, 2014) gave very comparable results (Figure S4, supplemental section), which opens up questions regarding glycogen metabolism and segregation of mutations throughout all chromosome copies in *Synechocystis*.

Transcript accumulation during growth phase of *Synechocystis* PG

Next to the regulation of the carbon flux towards DHAP, the expression of the genes encoding for the 1,2-propanediol synthesis pathway is essential for activity. As no product could be detected before day 8 (Figure 5 A, B), we wanted to elucidate how the operon encoding the respective production pathway is expressed, especially in the non-productive phase. Thus a cultivation experiment under optimized conditions was performed, and next to biomass and product formation, also the transcripts of *mgsA*, *ydhD*, and *adh* (by northern blotting) and the corresponding proteins (by mass spectroscopy) have been measured. Accumulation of product was detected starting from day 8, when the culture enters the late growth phase. The production rate increases slightly with biomass, with a rather constant specific activity of approximately $1.8 \mu\text{mol g}_{\text{CDW}}^{-1} \text{h}^{-1}$ ($14 \text{ fmol cell}^{-1} \text{h}^{-1}$) until day 12 (Figure 5B). Starting with day 12 and the transition from late growth to the stationary phase, a significant increase in 1,2-propanediol production can be observed, with specific activities being almost 10× higher ($16.5 \mu\text{mol h}^{-1} \text{g}_{\text{CDW}}^{-1}$, $130 \text{ fmol h}^{-1} \text{cell}^{-1}$) than in the late growth phase. The corresponding Northern Blot is shown in Figure 5D. Hybridization with the housekeeping gene *rnpB* verified the overall quality of RNA isolation. The length of the operon is expected to be 2779 bp with *adh* being 1057 bp, *yqhD* 1164 bp, and *mgsA* 559 bp long. However, the predicted full-length

polycistronic mRNA was not detected by Northern Blot analysis. The bands derived from hybridization with the *adh* and *yqhD* probes are of varying size, ranging from 200 to 2000 nt indicating an instable full-length transcript. The hybridization with the *mgsA* probe resulted in a distinct band of approximately 550 nt suggesting stabilization of the 3' end of the transcript due to the addition of a terminator sequence at the end of the operon (Figure 5). The other transcripts seem to become more stable until day 8 of cultivation, which coincides well with the accumulation of the product. As neither methylglyoxal nor acetol accumulated in the culture we assume that, although we could not detect a stable full-length mRNA, diverging stability of the transcript was not limiting for production. In addition we made shotgun proteomics of *Synechocystis* PG at

Days 3.8, 5.9, 8.06, and 10.9. with the wildtype strain serving as negative control. Two biological replicates were analyzed. While it was not possible to detect *mgsA*, the other two proteins of the pathway *yqhD* and *adh* have been detected at all time points. Remarkably, they belong to the 1% with the highest abundance of all 1200 proteins detected (Table S1, supplemental section).

4. Discussion

Cyanobacterial biotechnology has the potential for sustainable production of chemicals using exclusively CO₂, sunlight, and water. Within the last 10 years, photoautotrophic cyanobacteria, mainly *Synechococcus* and *Synechocystis* strains, have been genetically modified to produce several industrial relevant precursors, including 2,3-butanediol (Oliver et al., 2013), n-butanol (Lan and Liao, 2012), isobutyraldehyde (Atsumi et al., 2009), glycerol (Savakis et al., 2015), and lactic acid (Angermayr et al., 2012; Varman et al., 2013). Future, successful implementation of cyanobacteria as “green cell factories” in the chemical industry requires extended understanding of the underlying regulation of carbon flux and especially of carbon partitioning between product and biomass. The previously mentioned recombinant strains

share a common feature, namely the production of significant amounts of product in the transition to and in the stationary phase. Also 1,2-propanediol production by *Synechococcus elongatus* PCC7942 showed this phenomenon of ‘non-growth coupled’ productivity (Li and Liao, 2013). However, the authors focused on the redox cofactor preference of the alcohol dehydrogenase converting acetol to 1,2-propanediol to maximize product titers. Changing from an NADH-dependent alcohol dehydrogenase to an NADPH-dependent enzyme increased the 1,2-propanediol titer significantly from 22 to 150 mg L⁻¹ (2 mM). The phenomenon of ‘non-growth’-related productivity was not addressed.

1,2-propanediol formation in the stationary phase of *Synechocystis* PG

Here, *Synechocystis* was chosen as a host strain for light-driven biocatalysis and special attention was focused on the optimization of process parameters. As in the examples discussed above, *Synechocystis* PG also produced 1,2-propanediol only in the late growth and stationary phase. Nitrate and phosphate limitation and gene expression were investigated as possible explanations for the missing production of 1,2-propanediol during the exponential and linear growth phases of *Synechocystis* PG. While Nitrate was clearly not limiting (data not shown), all phosphate present in YBG11 medium is taken up by the cells already in the beginning of cultivation (Figure 3). However, elevated phosphate concentrations (>100%) are not beneficial for product formation. Methylglyoxal synthase isolated from *E. coli* is known to be allosterically inhibited by 2 mM of phosphate (Saadat and Harrison, 1998), which could be an explanation for this observation. At low phosphate concentrations another factor comes into play. As shown, glycogen plays a crucial role for 1,2-propanediol production. Only at higher OD values of >10 formation of this storage compound was observed (Figure 2B). At phosphate concentrations of 75% and below the cultures do not reach such high OD values, indicating that this storage compound has not yet accumulated to a sufficient extend for 1,2-propanediol production.

From the transcriptional analysis it may be concluded that the transcript stability of the full-length RNA covering the whole operon is limiting 1,2-propanediol production, as it was not possible to detect full length transcripts of *yqhD* and *adh*. However, the respective proteins could be detected by mass spectroscopy at high abundance in all samples. Not so clear is the situation regarding methylglyoxal synthase *msgA*. Although the *msgA* transcript shows very stable in the Northern Blot, it was not possible to detect the corresponding protein by mass spectroscopy. MgsA is the smallest protein of the three, with an unfavorable trypsin fragmentation pattern, yielding mostly either rather large or very small peptides, or peptides with a high histidine content. This could hamper detection of the respective masses. Alternatively it could be that the protein is really absent from the culture, meaning that the *msgA* transcript is not translated and the conversion of the precursor di-hydroxyacetone phosphate to methylglyoxal is catalyzed by a host intrinsic enzyme. Future optimization of the expression cassette could involve the construction of separate transcriptional units for the three genes of the pathway in order to limit post-transcriptional events and to control the amount of each of the enzymes independently as was suggested by Savakis et al. (2013).

Improvement of 1,2-propanediol productivity with *Synechocystis* PG

CO₂ and light supply have been tuned to the needs of the production host via reaction engineering resulting in improving final product titers from 3 mM (228 mg L⁻¹, 9 mmol_C L⁻¹) to 8 mM (610 mg L⁻¹, 24 mmol_C L⁻¹). Changing from constant illumination to L/D regimes did not influence the production pattern (see Figure 1 Supplemental section). No product formation was observed in the dark or throughout the growth phase. Further improvements were achieved when cultivation conditions known to be optimal for glycogen synthesis were realized (Monshupanee and Incharoensakdi, 2014). A maximal product concentration of 12 mM (900 mg L⁻¹, 36 mmol_C L⁻¹) was reached, which is six times higher than any previously reported values (2 mM, Angermayr et al., 2015; Li and Liao, 2013). Similarly, the production rate was

increased by a factor of 4 ($55 \mu\text{mol g}_{\text{CDW}}^{-1} \text{h}^{-1}$ vs. , $14 \mu\text{mol g}_{\text{CDW}}^{-1} \text{h}^{-1}$). The production of ethanol (Gao et al., 2012), 2,3- butanediol (Oliver et al., 2013) and isobutyraldehyde (Atsumi et al., 2009) represent three benchmark processes in the field of cyanobacterial research. Ethanol could be produced with a rate of $238 \mu\text{mol g}_{\text{CDW}}^{-1} \text{h}^{-1}$ up to an exceptionally high titer of 120 mM. Butanediol was produced with a maximum rate of $177 \mu\text{mol g}_{\text{CDW}}^{-1} \text{h}^{-1}$ to a final titer of 26 mM, while the strain producing isobutyraldehyde reached rates of $26 \mu\text{mol g}_{\text{CDW}}^{-1} \text{h}^{-1}$ and produced a final titer of 15 mM (Angermayr et al., 2015). All three strains produced the major part of the final product concentration during the stationary phase. Approximately 60 mM of ethanol and 15 mM 2, 3-butandiol were produced during the stationary phase. 2, 3-butandiol was produced with a stable rate of 1.1 mM day^{-1} for 14 days. In the case of isobutyraldehyde, even 12.5 mM was produced in the stationary phase, almost 85% of the total product titer, with a stable rate of 1.8 mM day^{-1} for 6 days. In the case of *Synechocystis* PG, the productivity was stable for 5 days after it had reached the stationary phase, with an overall volumetric production rate of 2.1 mM day^{-1} .

Intracellular carbon distribution between biomass, glycogen and 1,2-propanediol

The tight regulation of the carbon flux during photoautotrophic growth may be a reason for the limited production rates achieved with photoautotrophic hosts so far. In our case, 1,2-propanediol synthesis stopped as soon as the glycogen pool was depleted. This indicates that the presence of glycogen might be necessary for cell maintenance and therefore for the stability of the biocatalyst. Manipulating glycogen synthesis in order to reduce flux to an alternative carbon sink did not have a beneficial effect on 1,2-propanediol synthesis. Instead of improving productivities, product titers were dramatically reduced with no influence on the setting of the productive phase. Synthesis of 1,2-propanediol seems to be closely linked to the intracellular utilization of glycogen. The syntheses of other fermentation products such as succinate and acetate as found in literature were also reported to be directly coupled to glycogen. In these

Accepted Preprint

cases, the carbon and energy is delivered by storage compounds without photosynthetic activity (Hasunuma et al., 2016). However, this approach differs from ours as it was conducted under dark, anoxic conditions. To elucidate from which source the carbon is channeled into the product 1,2-propanediol, isotopic labelling experiments will be conducted in the near future.

Conclusions

The influence of the carbon partitioning on biomass, storage compounds, and synthetic pathways is of primary interest for all photoautotrophic fermentation approaches. Redirection of the carbon flux towards the desired product is one key approach for large-scale application of this technology. However, our findings show that prevention of carbon flux to storage compounds not necessarily result in higher productivities. Synthesis and accumulation of storage compounds during photoautotrophic growth and fermentative production of value-added compounds from glycogen might also be one promising strategy.

Acknowledgement

We thank Anne-Kathrin Leisinger and Benjamin Scheer for their excellent technical assistance and Prof. Klaas J. Hellingwerf for kindly supplying *Synechocystis* sp. PCC6308 Δ glgC. The authors are grateful for using the facilities of the Centre for Biocatalysis (MiKat) at the Helmholtz Centre for Environmental Research-UFZ, supported by the European Regional Development Funds (EFRE - Europe funds Saxony) and the Helmholtz Association.

Conflict-of-Interest Statement

The authors declare no commercial or financial conflict of interest.

References

- Angermayr SA, Gorchs Rovira A, Hellingwerf KJ. 2015. Metabolic engineering of cyanobacteria for the synthesis of commodity products. *Trends Biotechnol.* **33**:352–361.
- Angermayr SA, Paszota M, Hellingwerf KJ. 2012. Engineering a cyanobacterial cell factory for production of lactic acid. *Appl. Environ. Microbiol.* **78**:7098–106.
- Atsumi S, Higashide W, Liao JC. 2009. Direct photosynthetic recycling of carbon dioxide to isobutyraldehyde. *Nat. Biotechnol.* **27**:1177–80.
- Bertani G. 1951. Studies on lysogenesis. I. The mode of phage liberation by lysogenic *Escherichia coli*. *J. Bacteriol.* **62**:293–300.
- Bridgwater A, Chinthapalli R, Smith P. 2010. Identification and market analysis of most promising added-value products to be co-produced with the fuels. *Ast. Univ.:*1–132.
- Gao Z, Zhao H, Li Z, Tan X, Lu X. 2012. Photosynthetic production of ethanol from carbon dioxide in genetically engineered cyanobacteria. *Energy Environ. Sci.*, 5, 9857.
- Dienst D, Dühning U, Mollenkopf HJ, Vogel J, Golecki J, Hess WR, Wilde A. 2008. The cyanobacterial homologue of the RNA chaperone Hfq is essential for motility of *Synechocystis* sp. PCC 6803. *Microbiology* **154**:3134–3143.
- Gibson DG, Young L, Chuang R-Y, Venter JC, Hutchison C a, Smith HO. 2009. Enzymatic assembly of DNA molecules up to several hundred kilobases. *Nat. Methods* **6**:343–345.
- Gründel M, Scheunemann R, Lockau W, Zilliges Y. 2012. Impaired glycogen synthesis causes metabolic overflow reactions and affects stress responses in the cyanobacterium *Synechocystis* sp. PCC 6803. *Microbiology* **158**:3032–43.
- Hasunuma T, Matsuda M, Kondo A. 2016. Improved sugar-free succinate production by *Synechocystis* sp. PCC 6803 following identification of the limiting steps in glycogen catabolism. *Metab. Eng. Commun.* **3**:130–141.
- Hopper DJ, Cooper RA. 1971. The regulation of *Escherichia coli* methylglyoxal synthase; a

new control site in glycolysis? FEBS Lett. **13**:213–216.

Huang H-HH, Camsund D, Lindblad P, Heidorn T. 2010. Design and characterization of molecular tools for a Synthetic Biology approach towards developing cyanobacterial biotechnology. Nucleic Acids Res. **38**:2577–93.

Lan EI, Liao JC. 2012. ATP drives direct photosynthetic production of 1-butanol in cyanobacteria. Proc. Natl. Acad. Sci. U.S.A. **109**:6018–23.

Li H, Liao JC. 2013. Engineering a cyanobacterium as the catalyst for the photosynthetic conversion of CO₂ to 1,2-propanediol. Microb. Cell Fact. **12**:4.

Marco-Urrea E, Paul S, Khodaverdi V, Seifert J, von Bergen M, Kretzschmar U, Adrian L. 2011. Identification and characterization of a Re-citrate synthase in Dehalococcoides strain CBDB1. J. Bacteriol. **193**:5171–5178.

Monshupanee T, Incharoensakdi A. 2014. Enhanced accumulation of glycogen, lipids and polyhydroxybutyrate under optimal nutrients and light intensities in the cyanobacterium *Synechocystis* sp. PCC 6803. J. Appl. Microbiol. **116**:830–838.

Oliver JWK, Atsumi S. 2014. Metabolic design for cyanobacterial chemical synthesis. Photosynth. Res. **120**:249–261.

Oliver JWK, Machado IMP, Yoneda H, Atsumi S. 2013. Cyanobacterial conversion of carbon dioxide to 2,3-butanediol. Proc. Natl. Acad. Sci. U.S.A. **110**:1249–54.

Pinto FL, Thapper A, Sontheim W, Lindblad P. 2009. Analysis of current and alternative phenol based RNA extraction methodologies for cyanobacteria. BMC Mol. Biol. **10**:79.

Saadat D, Harrison DHT. 1998. Identification of catalytic bases in the active site of *Escherichia coli* methylglyoxal synthase: Cloning, expression, and functional characterization of conserved aspartic acid residues. Biochemistry **37**:10074–10086.

Savakis PE, Angermayr SA, Hellingwerf KJ. 2013. Synthesis of 2,3-butanediol by *Synechocystis* sp. PCC6803 via heterologous expression of a catabolic pathway from

lactic acid- and enterobacteria. *Metab. Eng.* **20**:121–130.

Savakis PE, Hellingwerf KJ. 2015. Engineering cyanobacteria for direct biofuel production from CO₂. *Curr. Opin. Biotechnol.* **33**:8–14.

Savakis PE, Tan X, Du W, Branco dos Santos F, Lu X, Hellingwerf KJ. 2015. Photosynthetic production of glycerol by a recombinant cyanobacterium. *J. Biotechnol.* **195**:46–51.

Saxena RK, Anand P, Saran S, Isar J, Agarwal L. 2010. Microbial production and applications of 1,2-propanediol. *Indian J. Microbiol.* **50**:2–11.

Schipp CJ, Marco-Urrea E, Kublik A, Seifert J, Adrian L. 2013. Organic cofactors in the metabolism of *Dehalococcoides mccartyi* strains. *Phil. Trans. R. Soc. B* **368**: 20120321

Schuermans RM, Matthijs JCP, Hellingwerf KJ. 2017. Transition from exponential to linear photoautotrophic growth changes the physiology of *Synechocystis* sp. PCC 6803. *Photosynth. Res.* **132**:69–82.

Shcolnick S, Shaked Y, Keren N. 2007. A role for mrgA, a DPS family protein, in the internal transport of Fe in the cyanobacterium *Synechocystis* sp. PCC6803. *Biochim. Biophys. Acta* **1767**:814–9.

Stanier RY, Kunisawa R, Mandel M, Cohen-Bazire G. 1971. Purification and properties of unicellular blue-green algae (Order *Chroococcales*). *Bacteriol. Rev.* **35**:171–205.

Taroncher-Oldenburg G, Stephanopoulos G. 2000. Targeted, PCR-based gene disruption in cyanobacteria: inactivation of the polyhydroxyalkanoic acid synthase genes in *Synechocystis* sp. PCC6803. *Appl. Microbiol. Biotechnol.* **54**:677–680.

Varman AM, Yu Y, You L, Tang YJ. 2013. Photoautotrophic production of D-lactic acid in an engineered cyanobacterium. *Microb. Cell Fact.* **12**:117.

Williams JGK. 1988. [85] Construction of specific mutations in photosystem II photosynthetic reaction center by genetic engineering methods in *Synechocystis* 6803. *Methods Enzymol.* **167**:766–778.

- Van der Woude AD, Angermayr SA, Puthan Veetil V, Osnato A, Hellingwerf KJ. 2014. Carbon sink removal: Increased photosynthetic production of lactic acid by *Synechocystis* sp. PCC6803 in a glycogen storage mutant. *J. Biotechnol.* **184**:100–102.
- Yan Y, Lee C-C, Liao JC. 2009. Enantioselective synthesis of pure (R,R)-2,3-butanediol in *Escherichia coli* with stereospecific secondary alcohol dehydrogenases. *Org. Biomol. Chem.* **7**:3914–3917.
- Zhou J, Zhu T, Cai Z, Li Y. 2016. From cyanochemicals to cyanofactories: a review and perspective. *Microb. Cell Fact.* **15**:2.

Table I: Strains and plasmids used in this study

Strains	Description	ABs	Source
<i>Synechocystis</i> sp. PCC 6803	WT strain	-	(Pasteur Culture Collection of Cyanobacteria)
<i>Synechocystis</i> sp. PCC 6803 PG	<i>lacIQ</i> , P_{TRC} , <i>mgsA</i> , <i>yqhD</i> , <i>adh</i> integrated into <i>slr0168</i>	Km	(this study)
<i>Synechocystis</i> sp. PCC 6803 Δ <i>glgC</i>	gene knockout of <i>slr1176/glgC</i> by replacement through Sm resistance gene	Sm	(this study)
<i>Synechocystis</i> sp. PCC 6803 Δ <i>glgC</i> PG		Km, Sm	(this study)
<i>Escherichia coli</i> DH5 α	cloning strain	-	(Hanahan 1983)
Plasmids	Description	ABs	Source
pBluescript II SK(+)	Backbone for integration plasmid	Amp	(Agilent technologies)
pSEVA234	Source for <i>lac^{IQ}</i> , P_{TRC}	Km	(Standard European Vector Architecture platform)
pEX-K4- <i>adh</i>	source for secondary alcohol dehydrogenase from <i>C. beijerinckii</i>	Km	(this study, Eurofins genomics)
pBS_ <i>slr0168::TRC</i>	pBluescript II SK(+) containing homologous regions for integration into <i>slr0168</i> as well as <i>lac^{IQ}</i> , P_{TRC}	Km, Amp	(this study)
pBS_ <i>slr0168::TRC:adh:yqhD:mgsA</i>	pBluescript II SK(+) containing homologous regions for integration into <i>slr0168</i> as well as <i>lac^{IQ}</i> , P_{TRC} , <i>mgsA</i> , <i>yqhD</i> , <i>adh</i>	Km, Amp	(this study)

Table II: Oligonucleotides used in this study

Primer	5' Extension	Sequence	Binding Region
homI_fwd		CTATAGGGCGAATTGGGTACC	<u>CCTTTGACAACAATGTGGCCTG</u>
homI_rev		GCTTATCGATACCGTCGACCTCGAGT	<u>TCCATATAAAATCCCCGCCACTG</u>
homII_fwd		TCTAGAGCGGCCGCCACCGCGGG	<u>ACCAAGCCAATTTTCGTTTG</u>
homII_rev		CTAAAGGGAACAAAAGCTGGAGCT	<u>CCCGCTAAACCCACCTCTTGC</u>
<i>lacIQTRC</i> _fwd		TGGCGGGGATTTATATGGACTCGAGT	<u>CTAGGGCGGCGGATTTG</u>
<i>lacIQTRC</i> _rev		ACGAAATTGGGCTTGGTCCC	<u>CGCGCAGCGGAAAAGGACAACGC</u>
<i>mgsA</i> _fwd	TATACGAAGCCGCCCGCTAAATAGTGGAGGTGTTACCATGGA	ACTGACGACTCGCAC	
<i>mgsA</i> _rev		CCCAGTCACGACGCGGCCGCTTACTTCAGACGGTCCGCG	
<i>yqhD</i> _fwd	GCGGTTGTTATCCTGTAATAGTGGAGGTGTTACCATGAACA	ACTTTAATCTGCACACCCC	
<i>yqhD</i> _rev			<u>TTAGCGGGCGGCTTCGTATATAC</u>
<i>CBsadh</i> _fwd	ACACCCTAGGCCGCGGCCGC	TAGTGGAGGTGTTACCATGAAAGGGTTTGCCATGTTAG	
<i>CBsadh</i> _rev			<u>TTACAGGATAACAACCGCC</u>
<i>mpB</i> _fwd			<u>GAGTTAGGGAGGGAGTTGCGG</u>
<i>mpB</i> _rev		TAATACGACTCACTATAGGGGCACTGTCCTCACGCTCGC	
<i>glgC</i> _cut1_fwd		ATCACGAGGCCCTTTCGTCTTCAAGAATTCAATTCCGGTGAACCGTGC	
<i>glgC</i> _cut1_rev			<u>TTCGAAGTCAAGTTTAGAACCG</u>
<i>glgC</i> _cut2_fwd		GCGAGATCACCAAGGTAGTCGGCAAATAAGGGCCAGTTTCTTTCTCTCG	
<i>glgC</i> _cut2_rev		TCGATGATAAGCTGTCAAACATGAGAATTC	<u>TTTCTGCCCCCTTGCTCTGC</u>
<i>Sm</i> _fwd		CCTCGTTCTAAACTTGACTTCGAACTTGGACTCCTGTTGATAGATCC	
<i>Sm</i> _rev			<u>CTTATTTGCCGACTACCTTGGTG</u>

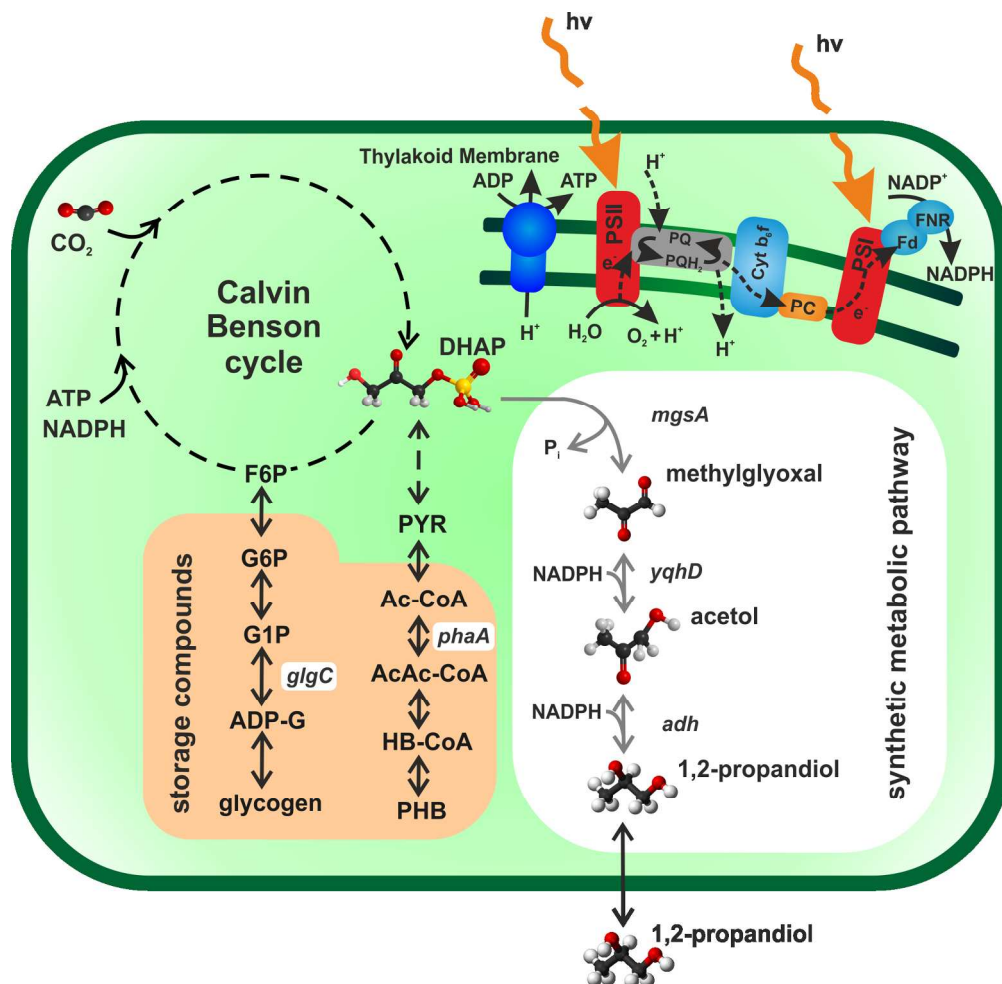


Figure 1: 1,2-propanediol pathway in *Synechocystis*. In a first step, methylglyoxal synthase (*mgsA*, derived from *E.coli*) converts the precursor dihydroxyacetone phosphate (DHAP) into methylglyoxal, which is subsequently reduced by a methylglyoxal reductase (*yqhD*, derived from *E.coli*) to acetol and then to 1,2-propanediol by a secondary alcohol dehydrogenase (*adh*, derived from *Clostridium beijerinckii*). Thereby two NADPH are consumed. In addition, pathways for the assembly of glycogen and PHB are shown and *glgC* and *phaA*, the genes mostly used for disruption of storage compound synthesis are highlighted.

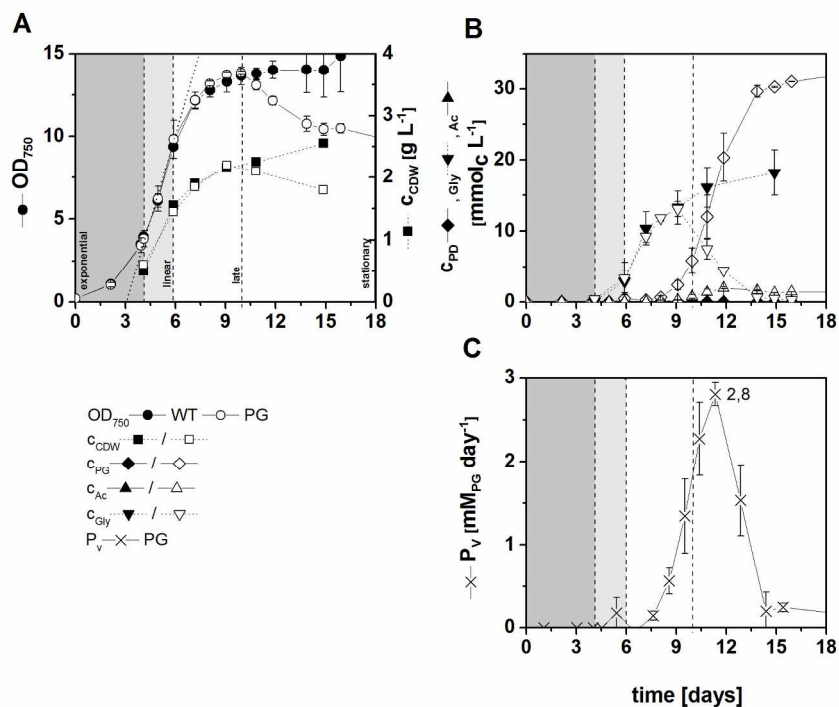


Figure 2: Growth and production parameters of the recombinant strain *Synechocystis* PG. (A) Growth of *Synechocystis* sp. 6803 PG (open symbols) in comparison to the wild type (solid symbols) (■-/- cCDW, ●-/- OD750). Note that the growth curves have not been corrected for the evaporation of the aqueous phase (0.2 mL day⁻¹) during the long cultivation times. **(B)** Glycogen turn-over (Gly), 1,2-propanediol (PD) and acetol (Ac) production in the respective strains. **(C)** Volumetric 1,2-propanediol productivity of *Synechocystis* PG over the time course of cultivation. Experiments were carried out in 250 mL baffled shaking flasks with a culture volume of 50 mL under increasing light intensity (25 – 200 μmol m⁻² s⁻¹, 2% CO₂, 30°C, 150 rpm, and 75% humidity in an INFORS Multitron photosynthesis plus incubator. With the exception of CDW, mean values and standard deviation of 4 biological replicates are shown.

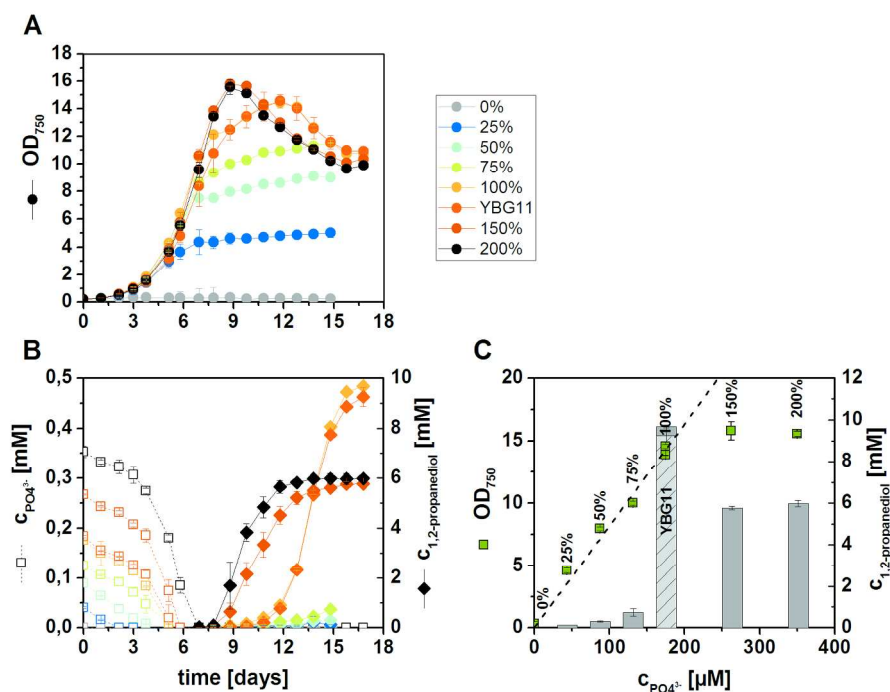


Figure 3: Influence of phosphate availability on growth of *Synechocystis* PG and 1,2-propanediol production. (A) Growth (OD₇₅₀) of *Synechocystis* PG cultures in YBG11 medium containing different phosphate concentrations relative to the standard phosphate content (0.175 mM) of YBG11 medium (0, 25, 50, 75, 100, 150, 200%). Note that the growth curves have not been corrected for the evaporation of the aqueous phase (0.2 mL day⁻¹) during the long cultivation times. (B) 1,2-propanediol production (filled symbols) in correlation to decreasing phosphate concentrations (open symbols). Color code given for panel A is also applicable for panel B. (C) Correlation of maximal OD₇₅₀ value to supplied phosphate concentrations and final 1,2-propanediol titers. Mean values and standard deviation of 2 biological replicates are shown.

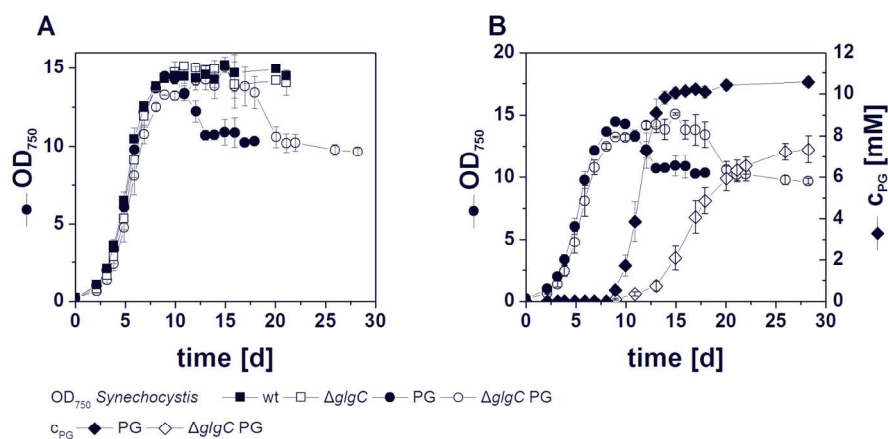


Figure 4: Growth and 1,2-propanediol production of *Synechocystis* PG compared to *Synechocystis* Δ glgC PG. (A) Growth of wt, PG, Δ glgC, and Δ glgC PG. (B) Growth and 1,2-propanediol production of PG (filled symbols) and Δ glgC PG (open symbols). Note that the growth curves have not been corrected for the evaporation of the aqueous phase (0.2 mL day^{-1}) during the long cultivation times.

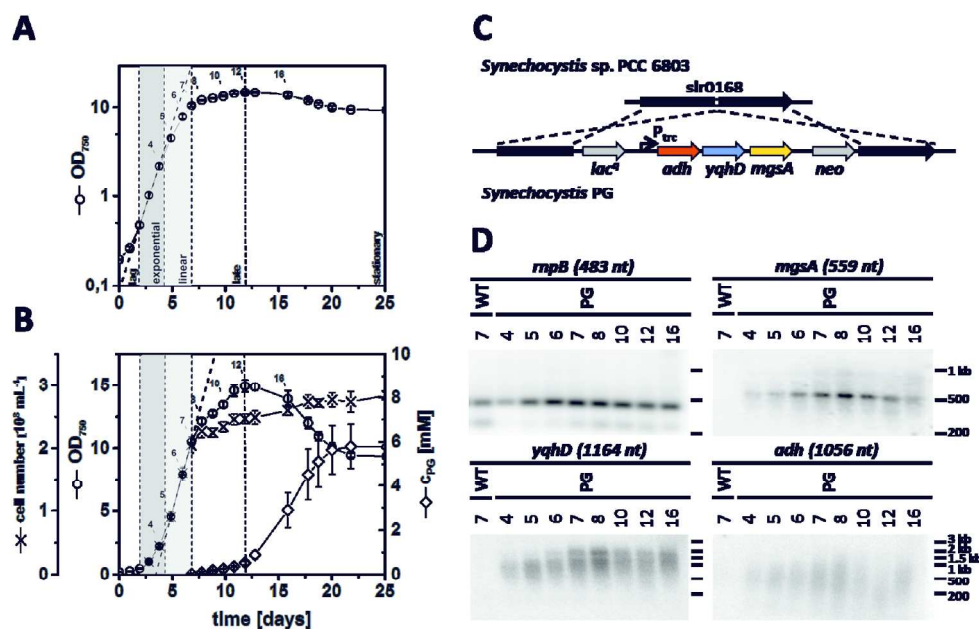


Figure 5: Analysis of 1,2-propanediol production pathway transcription by Northern Blot. (A)

Distinct growth phases of *Synechocystis* PG. **(B)** Growth (OD_{750} and cell number) and correlating 1,2-propanediol production. Note that the growth curves have not been corrected for the evaporation of the aqueous phase (0.2 mL day^{-1}) during the long cultivation times. **(C)** Scheme of the recombination cassette for the construction of *Synechocystis* sp. PCC 6803 TRC::adh:yqhD:mgsA **(D)** Northern Blot showing the transcript of the PG operon, using probes against the individual pathway mRNAs *adh*, *yqhD*, and *mgsA* during cultivation. DNA hybridization probes covered the complete coding region of the respective genes.

Timepoint of sampling is indicated in days. RNA quality and equal loading was checked using the housekeeping *mpB* gene. Wildtype RNA was used as a negative control.